HYPERTEMPORAL IMAGE ANALYSIS FOR CROP MAPPING AND CHANGE DETECTION

C.A. de Bie1), Mobushir R.Khan1), A.G.Toxopeus1), V.Venus1), A.K.Skidmore1)

1) ITC, P.O.Box 6, 7500 AA Enschede, The Netherlands
debie@itc.nl, khan@itc.nl, toxopeus@itc.nl, venus@itc.nl, skidmore@itc.nl

Commission VII, WG VII/5

KEY WORDS: Multitemporal, Change Detection, Mapping, Monitoring, Data Mining, SPOT, Crop, Land Cover

ABSTRACT:

Many authors explored the use of multi-temporal images, recorded within a season or across years, for (i) ecosystem monitoring, (ii) land cover (crop) identification, and (iii) change detection (Copin et.al, 2004). Temporary trajectory analysis, drawing on time-profile-based data originating from a large number of observation dates, has mainly been done through threshold-based methods, compositing-algorithms, or Fourier series approximation. This paper presents findings of a multivariate change detection method that processes the full dimensionality (spectral and temporal) of 10-day composite (1998-onwards) 1-km resolution SPOT-Vegetation NDVI images. Using the ISODATA clustering algorithm of Erdas-Imagine software and all available NDVI image data layers, unsupervised classification runs were carried out. These produced minimum- and average-divergence statistical indicators that in turn were used to identify the optimum number of classes that best suited the data put to the unsupervised classification algorithm. The selected classified map is linked to a set of time-profile-based signatures (profiles) that form the map legend. Studies were carried out for (i) Portugal to identify the extend and nature of land cover units, (ii) the Limpopo valley, Mozambique to map gradients, (iii) the Limpopo valley, Mozambique, to monitor flooded areas, (iv) Garmsar, Iran, to detect spatial differences in water availability, (v) Nizamabad, India, to link NDVI profiles to land use classes and (vi) Andalucía, Spain to disaggregate reported agricultural crop statistics to 1x1km pixel crop maps. Results compose of statistical findings underpinning the method, maps showing the spatial-temporal characteristics of the findings, and the applicability of the method for the studied topics.

1. INTRODUCTION

Land cover and land use studies often rely on maps derived from image interpretation coupled with field work. Images used represent mostly a single frame to cover the study area, or - at best – of a few repeats at different dates. Discussions frequently focus on resolution and scale. Agro-ecosystems however show frequently a higher temporal (seasonal) variability than a spatial one. This characteristic was in the past poorly used to support mapping due a lack of images. In recent years however, the use of NOAA-AVHRR, MODIS and SPOT-Vegetation data offered the option to study and gain insights of temporal dynamics due to their almost daily global revisiting frequency; this gain simultaneously implies a loss regarding spatial resolution (250m to 7km spatial resolution at a 10-daily availability of free synthesis products).

Traditionally, vegetation monitoring by remotely sensed data has been carried out using vegetation indices. These are mathematical transformations designed to assess the spectral contribution of green plants to multi-spectral observations (Maseli, 2004). A number of studies have shown that the normalised difference vegetation index (NDVI) derived by dividing the difference between infrared and red reflectance measurements by their sum provides effective measure of photosynthetically active biomass (Sarkar and Kafatos, 2004; Justice *et al*., 1985; Sellers, 1985; Drenge and Tucker, 1988; Ringrose *et al*. 1996; Maggi and Stroppiana, 2002; Weiss *et al*., 2004; Unganai and Kogan, 1998; Archer, 2004). Several studies also discussed the suitability of temporal NDVI profiles for studying vegetation phenologies, especially those of crops (Groten and Octare, 2002; Gorham, 1998; Hill and Donald, 2003; Uchida, 2001; Murakami *et al*., 2001).

Various authors have sought to map land-cover phenology, dynamics and degradation through multi-temporal NDVI data (e.g. Cayrol *et al*., 2000; Budde *et al*., 2004; Ledwith, 2000; Eerens *et al*., 2001; Brand and Malthus, 2004; Souza *et al*., 2003).

In this paper we explore an approach to utilise ten-day temporal resolution SPOT Vegetation data to identify (i) areas having different vegetation cover types and (ii) agricultural areas following different crop-calendars. The aim is to contribute to the development of compilation methods of spatial and temporal land-use data sets using existing data sources and improved RS/GIS-based methods.

2. DATA

Data available for this part of the study concern geo-referenced and de-clouded SPOT-4 Vegetation 10-day composite NDVI images (S10 product) at 1-km^2 resolution from April 1998 till present as obtained from www.VGT.vito.be. De-clouded means: using by image and pixel the supplied quality record; only pixels with a 'good' radiometric quality for bands 2 (red; 0.61-0.68 µm) and 3 (near IR; 0.78-0.89 µm), and not having 'shadow', 'cloud' or 'uncertain', but 'clear' as general quality, were kept (removed pixels were labelled as 'missing'). NDVI indicates chlorophyll activity and is calculated from (band 3 - band 2) / (band 3 + band 2).

3. METHOD

Using the ISODATA clustering algorithm of Erdas-Imagine software and all compiled and stacked NDVI image data layers, unsupervised classification runs were carried out to generate a map with a pre-defined number of classes. Unsupervised indicates that no additional data were used or expert's guidance applied, to influence the classification approach. The maximum number of iterations was set to 50 and the convergence threshold was set to 1.0. An iteration performed an entire classification, and was "self-organizing" regarding the way in which it located the clusters that are inherent in the data; the ISODATA algorithm minimizes the Euclidian distances to form clusters (Erdas, 2003; Swain, 1973). Of the produced map, selected NDVI-profiles (annual averaged profiles) are graphically presented and their spatial representation is shown. This paper will rely heavily on included figures to discuss the value of the chosen method.

4. RESULTS

4.1 West-Iberia: Area Stratification

Figure 1-top shows 45 generated NDVI profile classes and at the bottom 11 selected classes. For clarity, only annual averages of 7-year profiles are presented in the figure generated from 252 stacked images. The variation in behaviour between profiles differs considerably. The top-figure (red-arrow) suggests that around August a gradual gradient exists from rather low to very high NDVI values. This possibly relates to a weather defined gradient based on latitude and/or altitude.

Equally different is the area presented by each of the profiles (Figure 2). The presented map suggests a clear spatial stratification that is caused by a combination of weather, soil, terrain, and land use characteristics. It also presents distinct units that show remarkable homogeneity and at the same time locations where fragmentation of ecosystems occur. This logic can be reversed: the NDVI-profiles reflect and are good indicators of the environment in which the ecosystems occur. Use of the temporal dimension and NDVI values as an index for habitat / ecosystem functioning, provides an untapped stratification tool for mapping and monitoring. The down-side is that the product has a scale of 1:250.000 at best that consists of many ecosystem complexes compiled at a 1 km-sq spatial basis.

A key for effective monitoring and studying of natural resources is to define map units 'of interest' on the basis of their behaviour in time as can be detected by the chosen procedure. The following examples focus on various possibilities

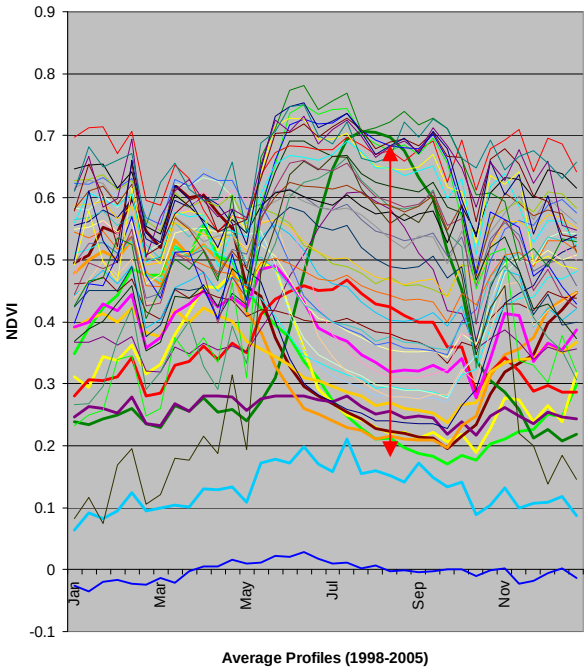

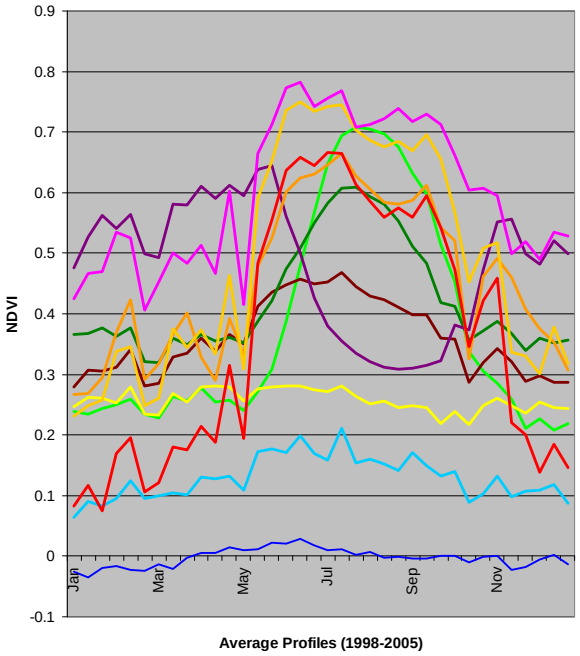

Figure 1 Top. All 45 NDVI-Profiles generated for the specified area,
Figure 1 Bottom. 11 Selected averaged annual SPOT NDVI-Profile classes (see Fig.2).

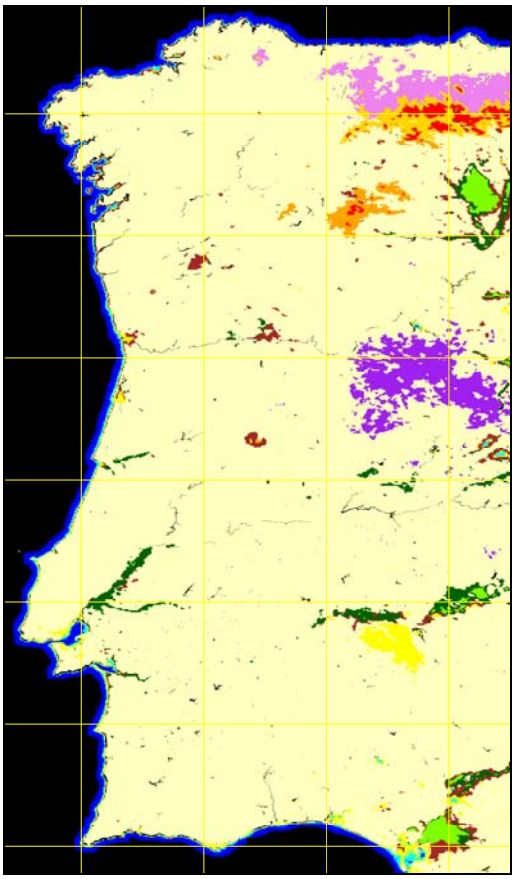

Figure 2. Spatial location of the shown 11 NDVI-Profile classes (see Figure 1).

4.2 Limpopo Valley, Mozambique: Gradient Mapping

On wind-blown sandy terraces along the coast of Mozambique, remnants of large-scale Cashew plantations can be found. After independence the plantations were abandoned and small parcels became property of local farmers who live under subsistence conditions in traditional villages scattered across the terraces. At present, management of the cashew is poor and selling surplus cashew-wood as charcoal on the local market generates most income. Progressive degradation of the tree-based land cover is widespread. Small land pockets exist where natural vegetation is allowed to become the dominant land-cover type because these areas are still contaminated by land mines.

An Aster image (Figure 3 top) shows that the vegetation density (in 2002) is far from homogeneous and that at the same time clear demarcation of land-cover map units is hard to establish. This is because three-cover can hardly be differentiated from other vegetated land-cover types (all red on the image). The zone consists of gradients that are partly caused by land factors and partly by its socio-economic history. The gradient can clearly be seen by comparing vegetated versus bare soil fractions across the area.

By running an unsupervised ISODATA clustering algorithm of stacked SPOT-Vegetation NDVI images (using a much larger window than the shown image extent), the area was stratified into 7 relatively homogeneous map units (Figure 3 bottom).

In Figure 4 it is interesting to note that the variability in NDVI (DN-values) over time (averaged yearly profiles) not only shows vegetation density differences by map-unit, but also that over time the behavior of the NDVI-profiles differs. Besides a gradient of vegetation density, the units also contain different mixes of vegetation types. Profiles that remain high over time, represent more permanent cover-types (trees) and curves that have reduced NDVI values, especially during the dry season (July-Nov), represent more degraded areas or fields (used for annual cropping). The gradient is best seen when comparing the September NDVI values between profiles. The difference in cover-types is best seen when comparing the general shapes of the curves. Profiles 45 and 43 remain high throughout the year: permanent cover of trees and undisturbed natural vegetation; profiles 22, 27 and 28 show clear dips during the dry season: a mix of trees and fields; profile 9 and 10 show considerably poorer NDVI values from April to July: fields and/or degraded cover-types are dominant.

Use of NDVI-images to capture the variability in time of cover types as present in an area to augment content derived from a single high-resolution image, proves thus relevant and required. Not only gradients can be delineated, but also meaning can be provided to what the gradients signify. Note that when required, the coarse resolution NDVI-map can be improved by re-delineating the given units with the support of the Aster image. The results show that besides the Aster image of May, an image around September is required to allow proper delineation of most relevant land-cover type complexes.

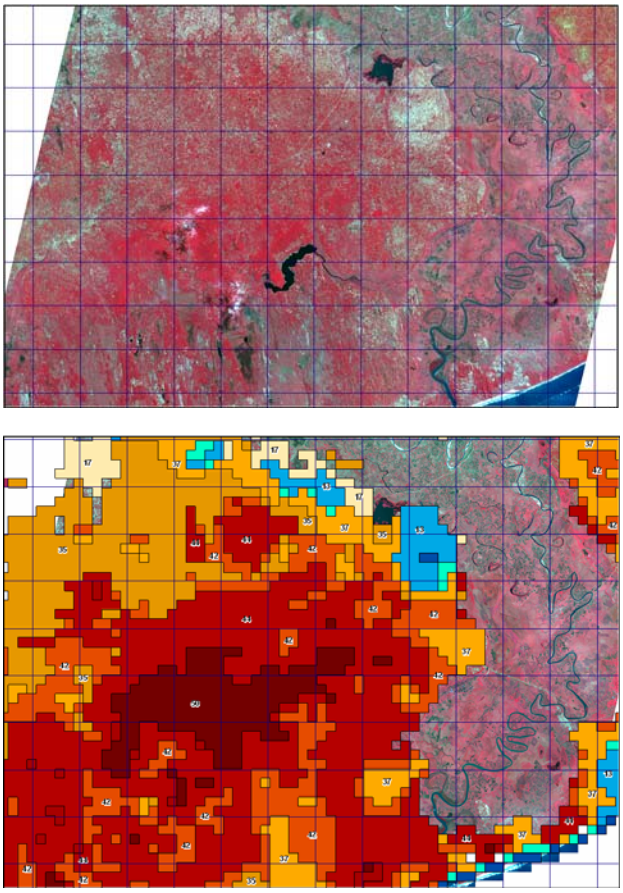

Figure 3 Top. Aster image of 10 May 2002 (RGB-b321) with a 5km grid showing sandy terraces left and right of the lower-Limpopo vally, Mozambique

Figure 3 Bottom. As above, with 10 SPOT-Vegetation NDVI classes displayed on top.

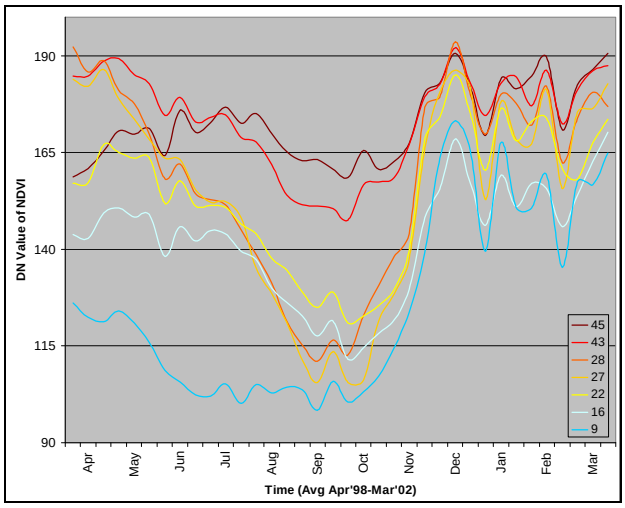

Figure 4. Legend of Figure 3: 7 NDVI profile classes.

4.3 Limpopo Valley, Mozambique: Flood Mapping

As in section 4.2 the Limpopo Valley is the area of interest. During the later part of the 20th century, the lower-floodplain of the Limpopo River is converted into an irrigation scheme demarcated by dams, irrigation structures and a regular pattern of large fields.

On the 15th of February 2000, after exceptional heavy rains and the passage of tropical cyclone 11S, main barriers upstream of the Limpopo river (located in S-Africa) had to be opened. This caused water levels to riserapidly, lower dams to break (Figure 5 top) and an overnight major flood to occur in the lower-floodplain of the Limpopo river (Figure 5). The SAR image shows clearly the extent of inundated areas one month after the major floods. Surplus water was only slowly drained to the sea due to the barrier of sand dunes aligning the coast (funnel effect).

Unsupervised stratification of stacked SPOT-Vegetation NDVI images covering three years and a larger extent as shown resulted in 6 NDVI based map units (Figure 5). The NDVI-profiles (Figure 6) were clearly classified on the basis of land-cover anomalies that occurred immediately after the floods. Land cover changed dramatically and recovered very gradually pending on the duration of inundation by area.

Local knowledge learned that unit 12 (dark brown) was inundated for a very short time-span (only days); its NDVI-profile shows only a minor dip. Units 15 and 7 were submerged for around one month (as confirmed by the SAR image); their NDVI-profiles showed considerable dips that recovered to normal after about 2-months. Units 10, 6 and 4 however remained for 1 to 3 months fully inundated (with standing water; Figure 6). Their NDVI-values dropped and remained below zero for months. Afterwards, the NDVI-profile of unit-6 shows a very strong vegetation growth beyond its normal density. It behaved like a swamp with excessive vegetation growth. This area is in reality not part of the irrigation scheme but consists of low-lying areas used for seasonal grazing. Unit 4 consists in reality of low-lying back-swamps where local farmers try to grow some sugarcane without any management. These remained like 'lakes' for 3 months. Only after 6 months their NDVI-values reached values of other classes.

Six months after the floods, due to severe inundation suffered, the whole area, but especially units 6 and 4, skipped the drop in NDVI as is normal during dry seasons (Jul-Nov). Clearly soils remained water-saturated well beyond the period required to drain all surplus standing water.

Use of NDVI-images to capture the variability in time of inundation as occurs in an area to augment other land use and land cover maps and/or to differentiate further responses to inundation, proves thus possible and meaningful. This applies to disaster areas but also to regular wetlands. Besides information that can be extracted using the temporal dimension, that dimension can thus also be used to delineate gradients of inundation and of related cover-types.

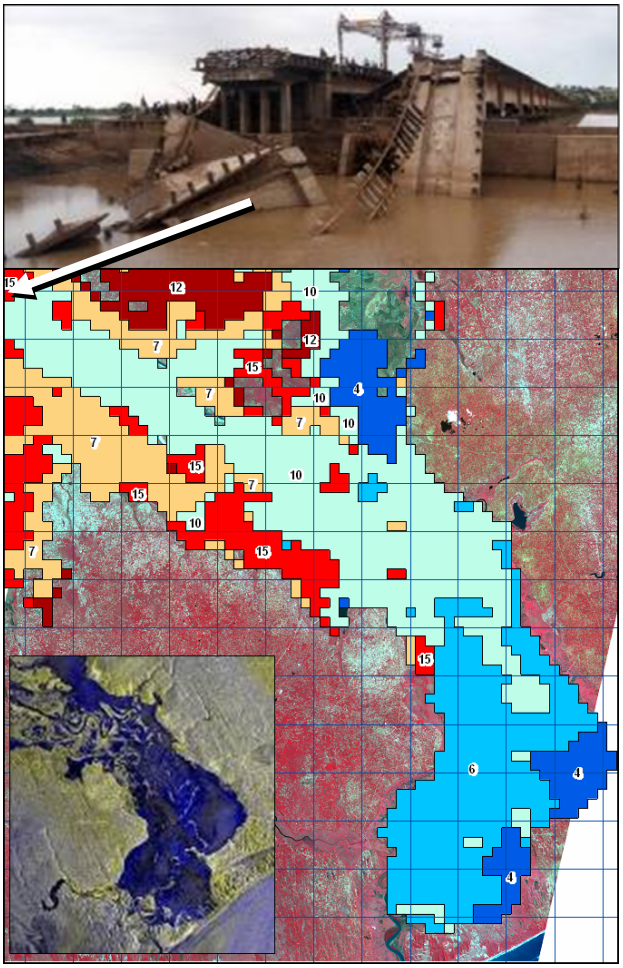

Figure 5. A main barrier dam north of Chokwe after the February 2000 floods, and below an Aster image with 6 SPOT-Vegetation NDVI classes displayed on top. As inset: a SAR image of 16 March 2000.

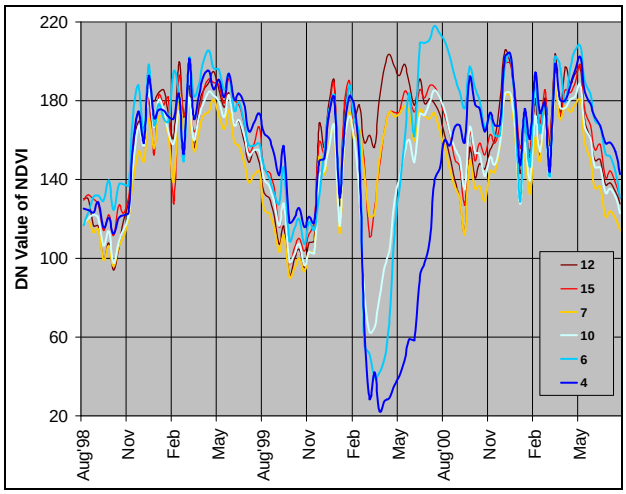

Figure 6. The legend of Fig.5, consisting of 6 NDVI profile classes.

4.4 Garmsar, Iran: Mapping Irrigation Water Supply

Garmsar, Iran, consists of an alluvial fan where 30 to 40 years ago an irrigation scheme was established (Figure 7 top). Use of a single Aster image and of data on followed crop calendars obtained through interviews with farmers, resulted in a detailed land-cover map as shown in Figure 7 (bottom). Using land-cover as of July 2001, a number of followed crop calendars could be differentiated, but only at the level of major land-use complexes. Data revealed that farmers exchange a fallow-year with a cropping year during which different crop-sequences are followed. Sharing the limited irrigation water rights between distinct canal command areas causes these changes. The presented land-cover map reflects land-cover at one point in time. It shows (see e.g. the fallow areas) the extent of distinct canal command areas. It could not be used to map agricultural land-use across years. For that purpose, the cover-map has a too limited validity in time.

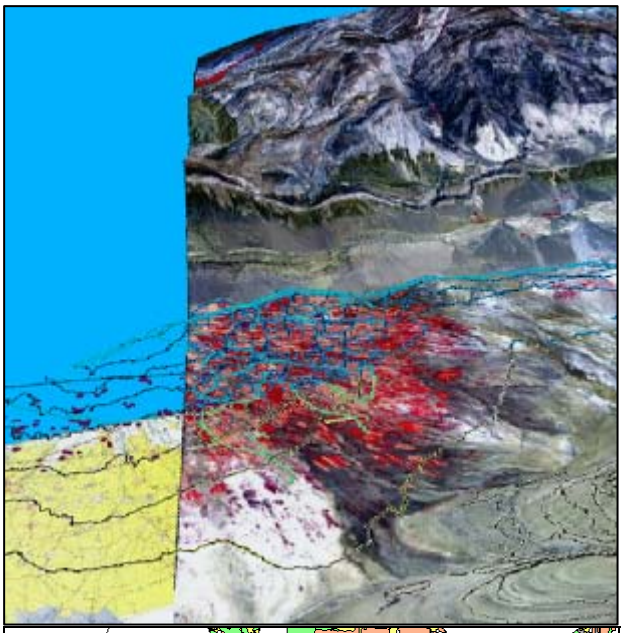

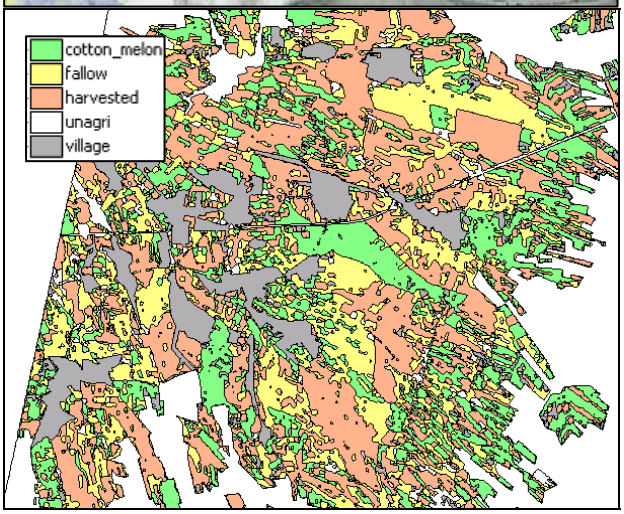

Figure 7 Top. Garmsar: 3D display of an Aster image (RGB-b321) of 30 July 2001 (based on the SRTD 90m DEM), with a topo-sheet at "zero" level and with contour lines,

Figure 7 Bottom. Aster image classification based on 43 interview data sets obtained from farmers.

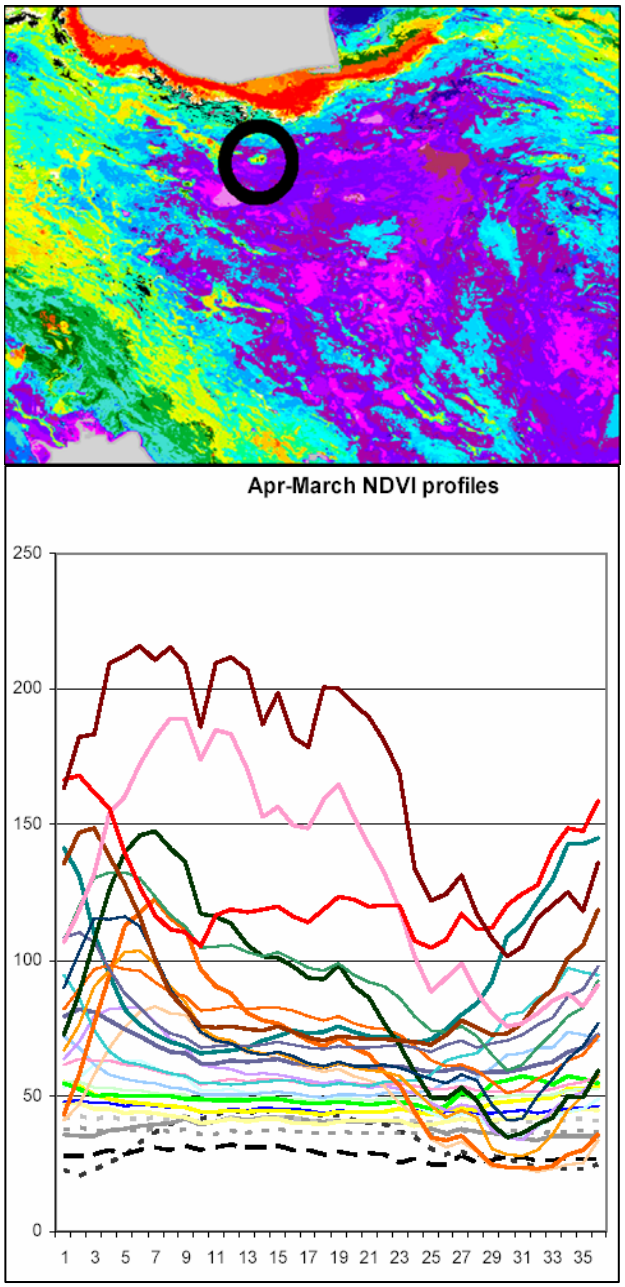

Figure 8 Top. 30 Unsupervised SPOT-Vegetation NDVI classes of Iran; Garmsar is marked by the circle,

Figure 8 Bottom. All generated annually averaged SPOT-Vegetation NDVI profiles (DN-values by April-March period).

Use of multi-year stacked SPOT-Vegetation NDVI data for Iran (Figure 8), led to an NDVI-map that differentiated 30 eco-systems on the basis of their NDVI-profiles. Zooming-in to Garmsar (Figures 9 and 10), showed that out of the 30 classes, 6 occurred in and around the irrigation scheme. The units showed particular spatial patterns. Units 22, 17 and 14 are aligned parallel to the irrigation scheme; unit 22 consists of a saline seepage zone (Figure 7 top) where limited vegetation grows (halophytes) from May to July (Figure 9 bottom). Unit 17 is intermediate between 22 and 14 where unit 17 consists of pure desert. Within the irrigation scheme units 19, 27 and 23 occur.

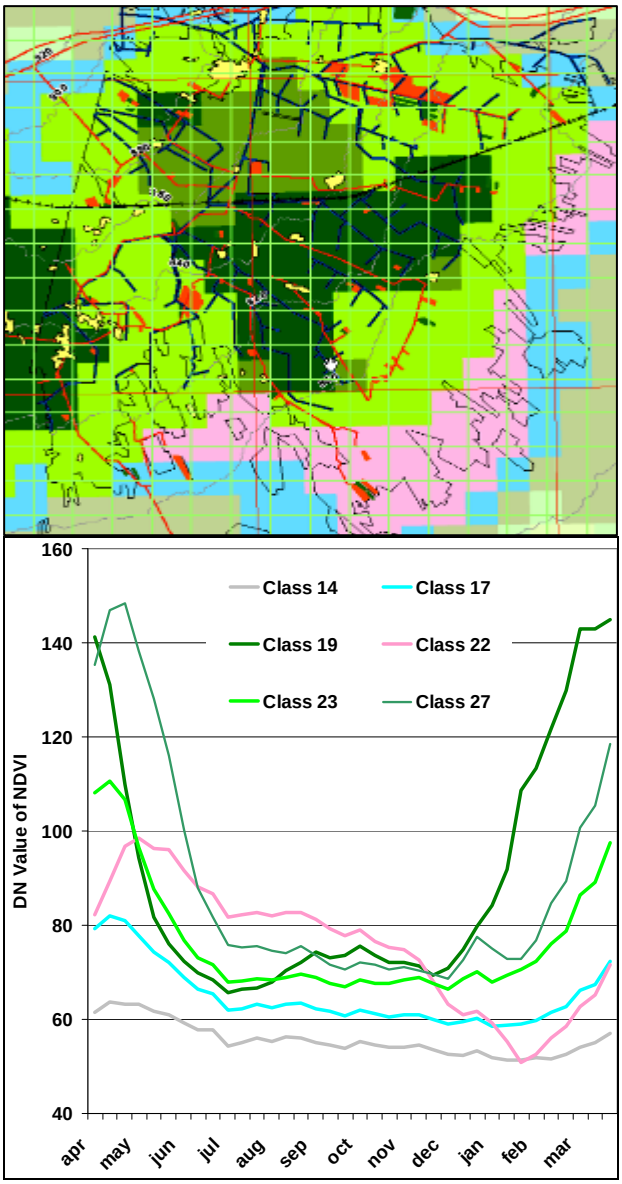

Figure 9 Top. Garmsar: Zoomed-in map based on Figure 8 showing 6 unsupervised SPOT-Vegetation NDVI classes,

Figure 9 Bottom. The 6 generated annually averaged SPOT-Vegetation NDVI profiles.

The centrally located unit (2 areas of unit 19; Figure 9 top), receives irrigation water early (already in Jan-March), and shows strong vegetation growth afterwards. Around it, areas of unit 27 are located. They show a delayed vegetation growth (Mar-May) of equal vigor; it clearly receives water after the primary areas are supplied sufficiently. The remaining areas of the irrigation scheme (unit 23) follow the NDVI-profile of unit 27, but only up to about half of the maximum shown NDVI values; it clearly suffers from water-shortage and on a 1 sq-km area basis, many fields must have remained fallow while others received what was available. The shown features were not reflected in the land-cover map derived from the Aster image (Figure 7 bottom).

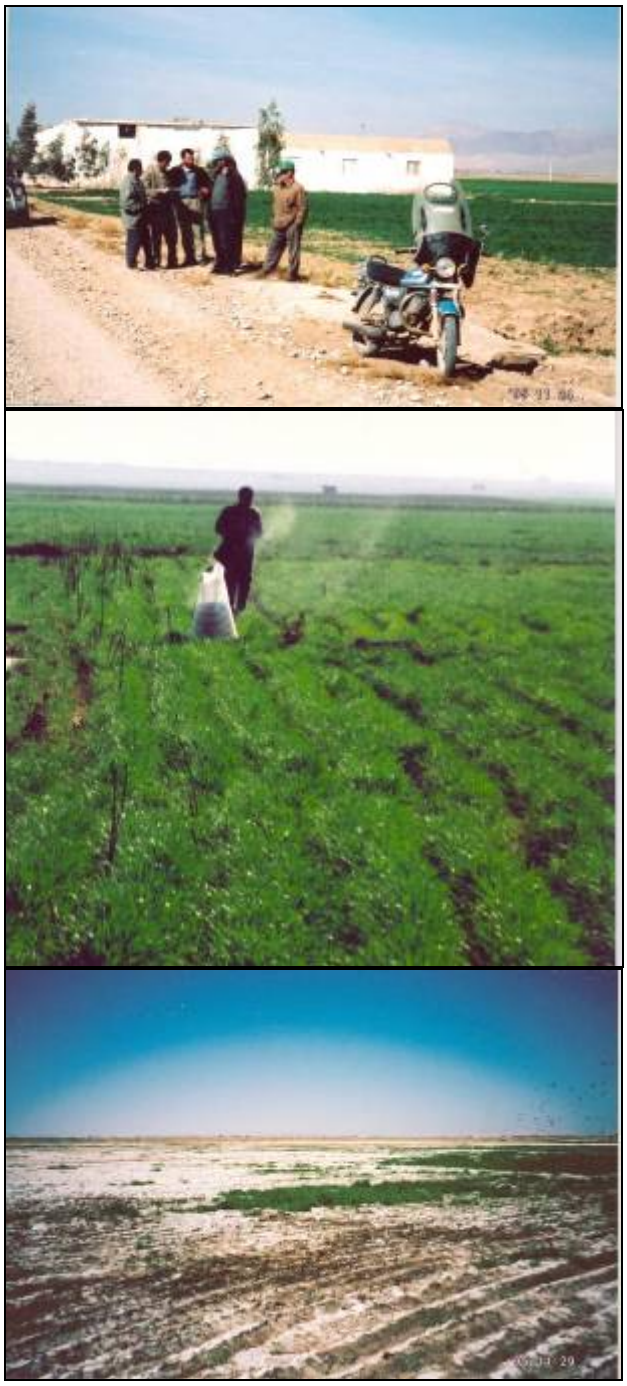

Figure 10. Impression of the Garmsar area.

Clearly use of multi-year hyper-temporal NDVI images revealed the 'larger' picture as occurs in the irrigation scheme studied. Annual variation was partly nullified by using images across years and partly by using a reduced scale. The validity and quality of content of the NDVI-map far exceeds the detailed Aster interpretation. In retrospect, organizing the fieldwork should have been based on the prepared NDVI map (through stratified sampling). Use of additional (multi-year) Aster images taken around March is suggested in case a better resolution map is required; use of a canal-command area map could have delivered additional value.

4.5 Nizamabad, India: Mapping and Monitoring Land Use

Nizamabad district, located in Hyderabad province, India, features an irrigation scheme used for rice cultivation, dry-land cropping on poor sandy soils and some cotton cultivation on vertisols that retain soil moisture beyond the wet monsoon period. Also degraded areas occur and hills covered with forests. The study area consisted of 6 Mandals (sub-districts).

Stacked Spot-Vegetation NDVI images covering 1998-2002 were subjected to the ISODATA unsupervised classification routine of Erdas-Imagine. Almost similar annual averaged NDVI-profiles were combined in order to reduce the number of classes and to remove inter-annual differences within the time-period studied. Figure 11 shows the resulting land unit map plus its legend. Further grouping of the classes was made on the basis of unit location and major shape of the NDVI-profiles concerned (see areas A, B, and C in Figure 11).

Using published crop-statistics by Mandal (in ha) and the area of each NDVI-class per Mandal (also in ha; see Table 1), by season (Kharif or summer and Rabi or winter) and crop, the following equation was estimated through step-wise multiple regression:

$$[\text{Cropped Area}_{\text{ by Mandal (ha)}} = f\,(\text{Area NDVI-Class}_{\text{ by Mandal (ha)}})]$$

No constant was used and regression coefficients were constraint to the 0 to 1 range.

Table 2 reports the results, e.g. [Cotton Area during summer (ha) = 0.148 for NDVI-Class ('7,8',9)], denoting that all 1 km-sq pixels of NDVI class '7,8' or 9 were estimated to represent a fraction of 14.8% of cotton during summer. The variability explained by all the 13 derived regression equations varied between 78 and 95%. In spite of the low available degrees of freedom (number of Mandals), all equations delivered significant coefficients (relations with NDVI-classes) and a high explanatory power (Adjusted-R^2). This success can only be explained if the derived NDVI-curves are strongly related to followed crop-calendars in the area and if those crop-calendars are sufficiently distinct. In area-A rice was dominant, in area-B pulses and groundnuts were found besides some maize and sugarcane, and in area-C pulses and sorghum were found besides some cotton. In degraded areas (unit '3,4,5,6') only sorghum was grown during summer on 25% of the area. As anticipated, the derived map consists of land-use complexes, since it has a scale of 1:250.000 at best.

After obtaining map units that clearly demarcate areas put to a known and distinct mix of land-uses, monitoring at unit level becomes like monitoring of pre-specified areas and land uses (cropping systems). Figure 12 provides an example. Area-A, representing NDVI-profiles '13,15', 17 and 18 is monitored during summer (49% irrigated rice) for 4 consecutive years. Within area-A the crop intensity (ratio of cropped to fallow fields) of unit-18 is high, of unit-17 average, and of unit '13,15' low. During the 3rd year, the disparity between the three units in crop-intensities increases, and during the 4th year all units showed a distinct drop in crop intensities. Local knowledge revealed that during the 2001 monsoon, India suffered from major droughts and farmers were faced with load shedding (only a few hours of electricity supply per day). Because most paddy fields (rice) are irrigated by submerged pumps run by

electricity, farmers decided to increase the area kept fallow so that sufficient water could be pumped for fields cropped. Yields per hectare may not have dropped, but the total production for the concerned districts did.

The data-mining exercise, converting published crop-area statistics to a land-use map proved feasible through the intermediate use of hyper-temporal NDVI images. The quality to map different cropped areas and the explanatory power of the equations that estimate the fractions cropped by sq-km proved very robust. Using the delineated areas for monitoring will likely be used for future generations of monitoring methods.

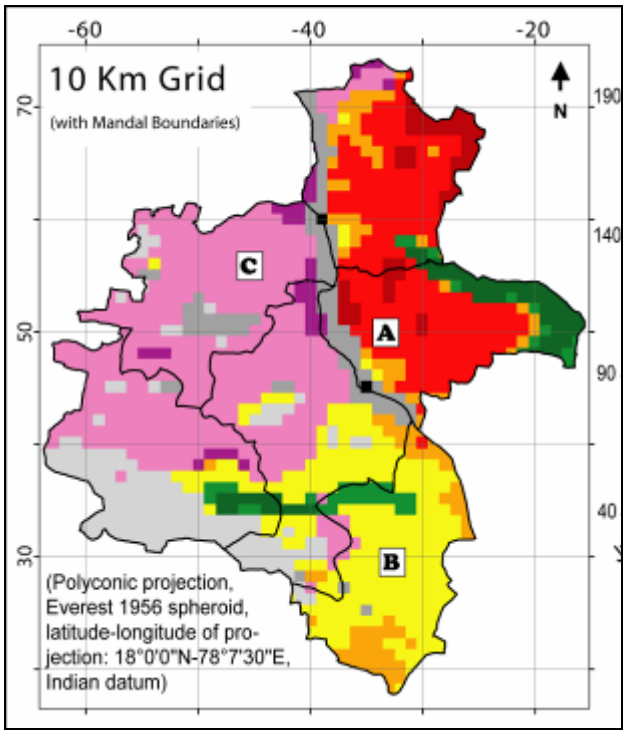

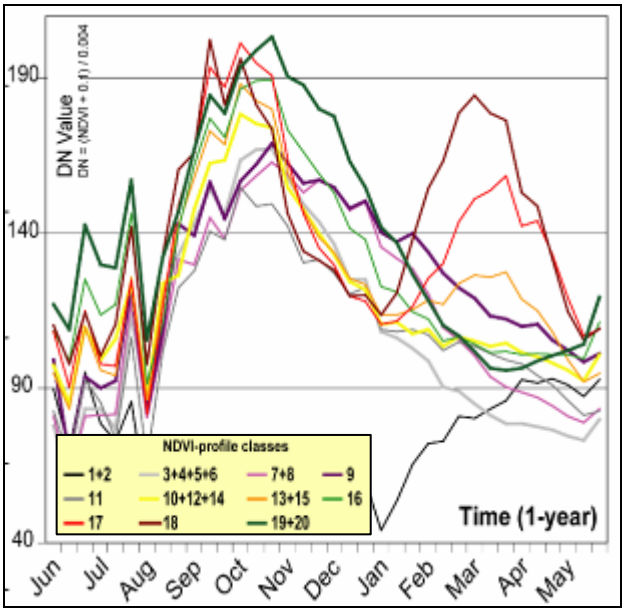

Figure 11. 1-km2 NDVI-unit map with 11 NDVI-profiles as preliminary legend. Area A: Classes '13, 15', 17 and 18 (brown, red, orange), Area B: Class '10, 12, 14' (yellow), Area C: Classes '7, 8' and 9 (light and dark purple).

KHARIF	Bichkunda	Birkoor	Jukkal	Kotagir	Madnoor	Pitlam	Total(ha)
Irrig.Rice	3,255	6,919	793	7,325	1,282	3,200	22,774
Sorghum	718	4	2,305	1	371	564	3,963
Maize	12	27	52	7	0	384	482
Pulses	5,986	93	6,609	1,312	9,268	5,853	29,122
Sugarcane	230	372	4	951	64	774	2,395
Cotton	628	11	2,524	313	2,910	474	6,860
Other Crops	218	16	518	151	150	50	1,103
Total(ha)	11,047	7,442	12,805	10,060	14045	11,299	66,699

RABI	Bichkunda	Birkoor	Jukkal	Kotagir	Madnoor	Pitlam	Total(ha)
Irrig.Rice	651	3,995	247	4,153	335	2,100	11,481
Sorghum	2,462	16	3,035	1,181	6,987	1,773	15,454
Millet	0	4	0	34	0	0	38
Maize	6	10	0	0	0	61	77
Pulses	885	4	368	243	1,001	323	2,823
Sugarcane	245	244	0	803	0	668	1,960
Groundnut	657	820	469	1,205	658	2,133	5,942
Other Crops	1,153	187	1,771	337	1,966	433	5,847
Total(ha)	6,059	5,280	5,890	7,956	10,947	7,490	43,622

NDVI-Profile Class*	Bichkunda	Birkoor	Jukkal	Kotagir	Madnoor	Pitlam	Total(km^2)
1,2	0	1	0	1	0	0	2
11	16	18	2	16	28	2	81
3,4,5,6	33	0	91	0	10	3	136
19,20	4	34	9	3	0	0	50
16	3	8	6	3	0	15	34
10,12,14	71	2	17	3	1	140	234
7,8	112	0	105	13	173	4	407
9	8	1	5	6	10	0	29
13,15	7	15	1	30	0	38	91
17	0	109	0	102	0	1	212
18	0	12	0	28	0	0	40
Total (km^2)	254	200	237	204	222	202	1,318

* Product of the image classification step discussed under 'methods'.

Table 1. Crop statistics for 6 Mandals; three-year averages (1998/99-2000/01; ha), and total area of NDVI-profile classes in each Mandal (km^2)

		NDVI-profile Class Groups				
			Area B:	Area C:	Area A:	
KHARIF	Adj.R^2	3,4,5,6	10,12,14	'7,8',9	'13,15',17,18	Area (ha)
Irrig.Rice	88%				49.6%	22,774
Sorghum	95%	25.2%				3,963
Maize	78%		2.2%			482
Pulses	95%		34.0%	46.6%		29,122
Sugarcane	89%		3.9%		4.6%	2,395
Cotton	82%			14.8%		6,860
Other crops	89%	5.9%				1,103

RABI	Adj.R^2	3,4,5,6	10,12,14	'7,8',9	'13,15',17,18	Area (ha)
Irrig.Rice	95%				28.4%	11,481
Sorghum	89%			32.2%		15,454
Pulses	87%			5.6%		2,823
Sugarcane	85%		3.6%		3.6%	1,960
Groundnut	88%		12.6%		6.7%	5,942
Other crops	92%			11.7%		5,847
Area (km^2)		136	234	436	343	

Note: the Adjusted R2, when regression through the origin is forced, cannot be compared to R2s for models that include an intercept.

Table 2. Results of the multiple stepwise linear regression analysis. Reported cropped areas are estimated by the extent of NDVI-profile classes. Coefficients are reported as percentages that are confined to the 0-100% range (0 to 1); each was significance at 5%

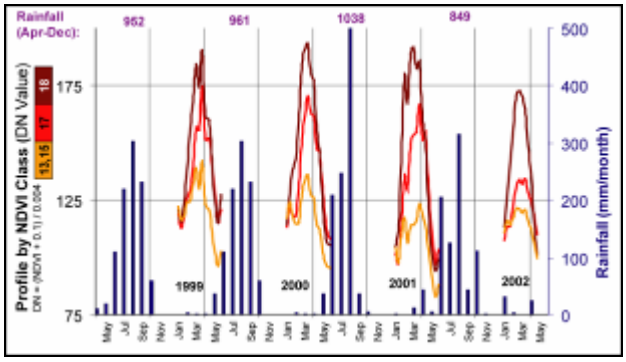

Figure 12. Monitoring land-use modifications: Monthly rainfall (plus seasonal totals) is compared to NDVI-profiles of irrigated areas where during Rabi the dominant crop is rice.

4.6 Andalucía, Spain: Generating Crop Maps

Like in paragraph 4.5, step-wise multiple regression is used to convert published crop area statistics to a land unit map. This exercise is included (i) to focus on optimizing the number of classes generated through the unsupervised ISODATA clustering method of Erdas, and (ii) to evaluate the product on the basis of extensive fieldwork data generated by the Andalucían Government.

Figure 13 shows both the location of Andalucía in Spain as the location of agricultural areas within Andalucía. The latter product was generated from the Corine 2000 land cover map. Using the ISODATA clustering method of Erdas, 9 years of stacked NDVI images were classified to a range of pre-set classes (10 to 100; Figure 14). Using the generated statistics by classification run, divergence statistics were extracted expressed in 'separability values'. The minimum separability denotes the similarity between the two most similar classes, and the average separability denotes the similarity amongst all classes; both should be as high as possible while the number of classes should remain limited. Figure 14 is used to evaluate for which pre-set number of classes a natural balance is established, i.e. it helps decide on the number of meaningful classes that can be differentiated for the studied dataset on the basis of information hidden in it. The figure reveals clearly the reason why the choice was made for the 45 classes map. Figure 15 shows the 45 classes map for agricultural areas only (ref. figure 13).

Using published crop-statistics by municipality (in ha; for 2397 municipalities) and the area of each NDVI-class per municipality (also in ha), the following equation was estimated through step-wise multiple regression for rainfed wheat:

$$[\text{Cropped Area}_{\text{ by Municip.(ha)}} = f(\text{Area NDVI-Class}_{\text{ by Municip.(ha)}})]$$

No constant was used and regression coefficients were constraint to the 0 to 1 range.

Table 3 reports the established equation. It states by NDVI-class the fraction per sq-km cropped to rainfed wheat. 8 NDVI-classes represented > 10% rainfed wheat per sq-km (upto 47%) and 7 NDVI-classes represented < 10% rainfed wheat per sq-km. All derived coefficients were highly significant and the explained variability was 98.8% (Adjusted-R^2).

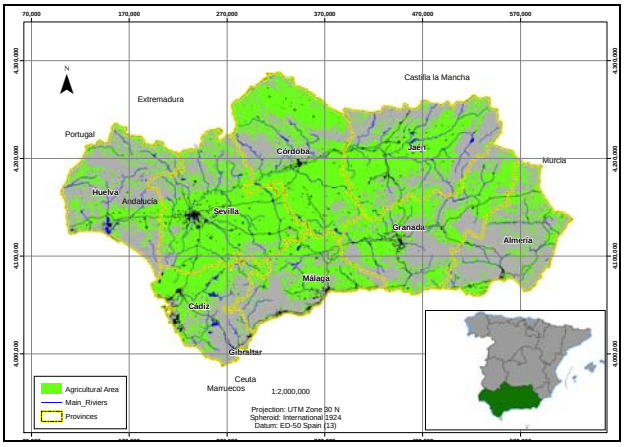

Figure 13. Agricultural Areas in Andalucía, Spain, according to the Corine Land Cover 2000 map.

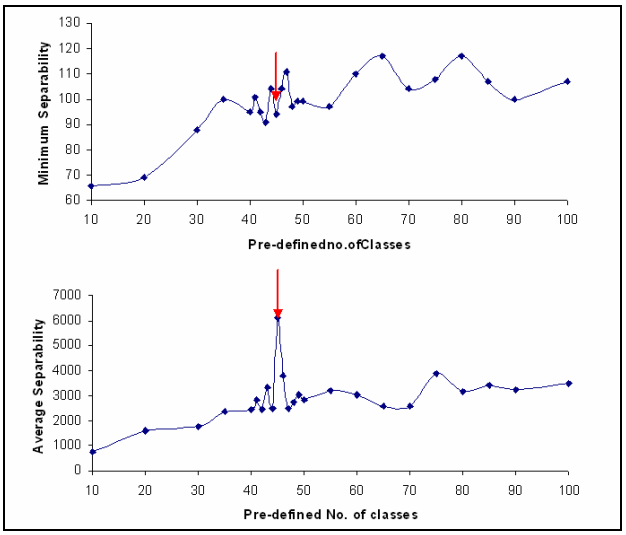

Figure 14. Divergence Statistics (Avg. and Min.) to identify the optimal number of classes (=45) to run an unsupervised ISODATA stratification of 9 years decadal SPOT-Vegetation NDVI images (April'98-06; 324 stacked layers).

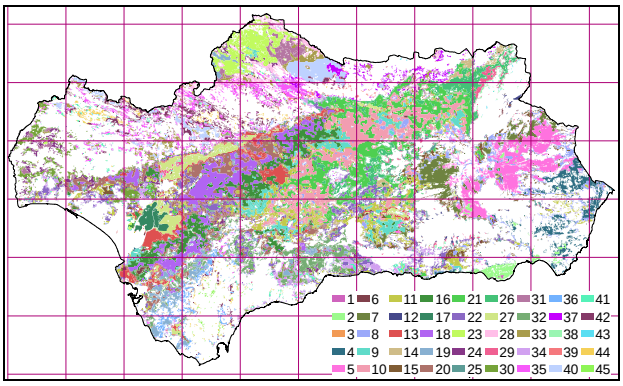

Figure 15. 45 SPOT-Vegetation NDVI Classes of the Agricultural Areas of Andalucía, Spain

Using the regression equation and the NDVI-classes map, a rainfed wheat map is made (Figure 16). The mono-thematic

map shows within the agricultural areas of Andalucía, independent of municipality boundaries, where rainfed wheat is grown, as fractions of 1 sq-km areas. Figure 17 shows the NDVI-profiles of NDVI-classes that represent > 10% rainfed wheat per sq-km. Especially profiles '18,19' and 16 relate to wheat, the other three profiles include other land cover types as can be seen by their relatively high NDVI-values during the January-March period. Besides these differences, the vigor of the class '19,20' is better than class 16, while both represent about the same fractions of rainfed wheat per sq-km (47 and 42%); this points to a difference in performance at field-level.

Figure 18 shows the location of 1451 700x700m segments of which about half are annually visited by the Government of Andalucía to survey by field the type of crop grown. From the 2001-05 dataset, by year, the actual fraction cropped to rainfed wheat within each segment could be extracted. After linking the centroids of each segment (with their attribute data) to the NDVI map, validation and variability data could be generated. The count of segments by NDVI-class was used as a weight factor to complete the validation process. The regression equation was forced through the origin.

NDVI Class No	Coefficients	t	Sig.
18	0.468	55.1	0.000
19	0.466	25.2	0.000
16	0.420	58.1	0.000
23	0.335	53.7	0.000
20	0.287	23.1	0.000
36	0.268	8.7	0.000
9	0.266	24.0	0.000
31	0.118	6.4	0.000
7	0.093	8.0	0.000
24	0.084	2.9	0.004
5	0.081	13.2	0.000
35	0.079	5.7	0.000
22	0.070	5.3	0.000
27	0.064	4.9	0.000
10	0.024	3.6	0.000

Table 3. Results of Step-Wise Forward Multiple Regression to Estimate Fractions of Rainfed Wheat per Sq-km (Ad justed-R^2 of 0.988)

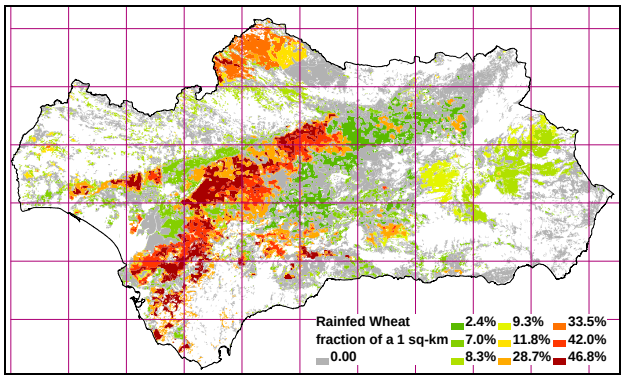

Figure 16. Crop-map with a 50km grid for Rainfed Wheat in fractions per sq-km as located within Agricultural Areas of Andalucia, Spain.

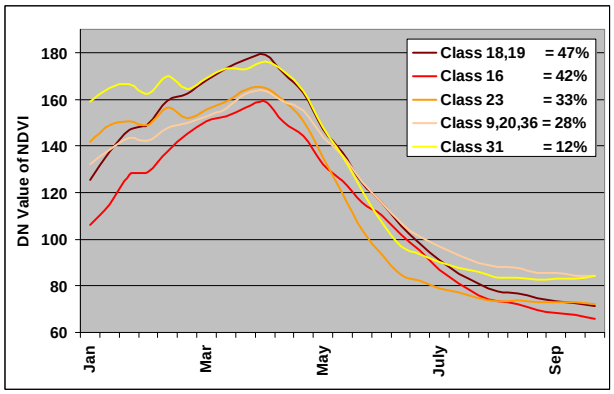

Figure 17. SPOT-Vegetation NDVI Profiles for Classes having > 10% Rainfed Wheat.

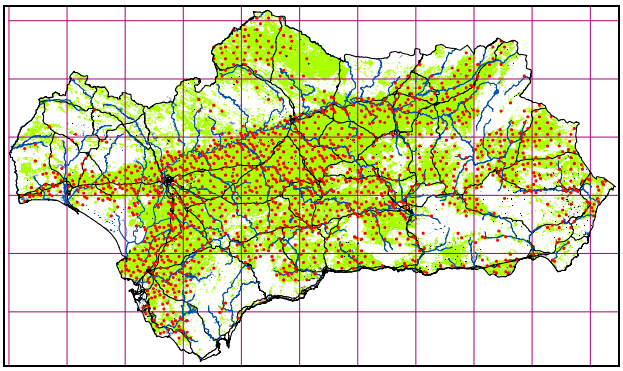

Figure 18. Location of the Validation Data Set consisting of 700x700m segments surveyed from 2001-05.

Figure 19 shows that the validation explained 45% of the total variability and the regression line is close to the 1:1 ratio line. The variability between segments of a single NDVI-class remained high (see box-whiskers), indicating that the map of Figure 16 still has a considerable amount of generalisation. Variability between units seems optimized though still considerable variability remains within units.

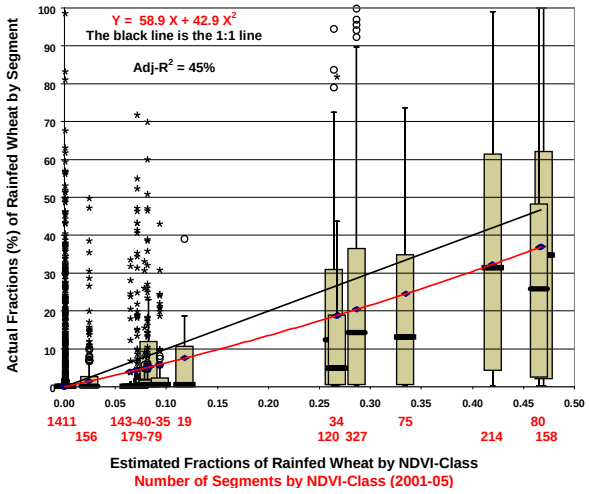

Figure 19. Validation of the NDVI-based Rainfed Wheat Map using the Fractions of Rainfed Wheat of 3272 Segments (2001-05 dataset). Presented are box-whiskers by NDVI-Class and a 2nd polynomial regression line.

REFERENCES

ARCHER E.R.M., 2004, Beyond the "climate versus grazing" impasse: using remote sensing to investigate the effects of grazing system choice on vegetation cover in the eastern Karoo. *Journal of Arid Environments* **57**: 381-408.

BRAND S. and MALTHUS T.J., 2004, Evaluation of AVHRR NDVI for monitoring intra-annual and interannual vegetation dynamics in a cloudy environment (Scotland, UK). In: *Proceedings of the XXth ISPRS Congress*, Commission-II, 12-23 July 2004 Istanbul, Turkey. 6pp.

BUDDE M.E., TAPPAN G., ROWLAND J., LEWIS J. and TIESZEN L.L., 2004, Assessing land cover performance in Senegal, West Africa using 1-km NDVI and local variance analysis. *Journal of Arid Environments* **59**: 481-498.

CAYROL P., CHEHBOUNI A., KERGOAT L., DEDIEU G., MORDELET P. and NOUVELLON Y., 2000, Grassland modelling and monitoring with SPOT-4 Vegetation instrument during the 1997-1999 SALSA experiment. *Agricultural and Forest Meteorology* **105**: 91-115.

Coppin P., Jonckheere I., Nackaerts K., Muys B., Lambin E., Review Article. Digital change detection methods in ecosystem monitoring: a review. *International Journal of Remote Sensing*, **25:9**, 1565 – 1596.

DRENGE H.E. and TUCKER C.J., 1988, Green biomass and rainfall in semi-arid sub-Saharan Africa . *Journal of Arid Environments* **15**: 245-252.

EERENS H., KEMPENEERS P., PICCARD I. and VERHEIJEN Y., 2001, Crop monitoring and yield forecasting with NOAA-AVHRR or SPOT-Vegetation. http://www.geosuccess.net/ geosuccess/documents/Dry_Matter_Productivity.pdf (accessed 21 Apr'08).

ERDAS, 2003, ERDAS Field Guide. 7th ed. *GIS & Mapping*, LLC Atlanta, Georgia & Leica Geosystems GIS & Mapping, LLC. 698 pp.

GORHAM B., 1998, Mapping multi-temporal agricultural land use in Mississippi Alluvial valley of Arkansas. In: *Proceedings of the Spatial Technologies in Agricultural and Natural Resources*: SRIEG-10 Annual Conference, Global Hydrology and Climate Centre, Huntsville, USA.

GROTEN S.M.E.and OCATRE R., 2002, Monitoring the length of the growing season with NOAA. *International Journal of Remote Sensing* **23**.14: 1271-1318.

HILL M.J. and DONALD G.E., 2003, Estimating spatio-temporal patterns of agricultural productivity in fragmented landscapes using AVHRR NDVI time series. *Remote Sensing of Environment* **84**: 367-384.

JUSTICE C.O., TOWNSHEND J.R.G., HOLBEN B.N. and TUCKER C.J., 1985, Analysis of the phenology of global vegetation using meteorological satellite data. *International Journal of Remote Sensing* **6**: 1271-1318.

Ledwith, M., 2002. Land cover classification using SPOT Vegetation 10-day composite images - Baltic Sea Catchment basin. *GLC2000 Meeting*, Ispra, Italy, April 18-22.

MAGGI M. and STROPPIANA D., 2002, Advantages and drawbacks of NOA-AVHRR and SPOT-VGT for burnt area mapping in a tropical savannah ecosystem. *Canadian Journal of Remote Sensing* **28**.2: 231-245.

MASELI F., 2004, Monitoring forest conditions in a protected Mediterranean coastal area by analysis of multiyear NDVI data. *Remote Sensing of Environment*. **89**: 423-433.

MURAKAMI T., OGAWA S., ISHITSUKA N., KUMAGAI K. and Saito G., 2001, Crop discrimination with multi-temporal SPOT/HRV data in the Saga Plains, Japan. *International Journal of Remote Sensing* **22**.7: 1335-1348.

RINGROSE S., VANDERPOST C. and MATTHESON W., 1996, The use of integrated remotely sensed and GIS data to determine the causes of vegetation cover change in: southern Botswana. *Applied Geography* **16**: 225-242.

SARKAR S. and KAFATOS M., 2004, Inter-annual variability of vegetation over the Indian sub-continent and its relation to the different meteorological parameters. *Remote Sensing of Environment* **90**: 268-280.

SELLERS P.J., 1985, Canopy reflectance, photosynthesis and transpiration. *International Journal of Remote Sensing* **6**: 1335-1372.

SOUSA, C.Jr., FIRESTONE L., SILVA L.M. and ROBERTS D., 2003, Mapping forest degradation in the eastern Amazon from SPOT 4 through spectral mixture models. *Remote Sensing of Environment* **87**: 494-506.

SWAIN P.H., 1973, *Pattern Recognition: A Basis for Remote Sensing Data Analysis* (LARS Information Note 111572). The Laboratory for Applications of Remote Sensing, Purdue University, West Lafayette, Indiana.

UCHIDA S., 2001, Discrimination of Agricultural Land use using mulit-temporal NDVI data. In: *Proceedings of 22nd Asian Conference of Remote Sensing*. Singapore, Centre for Remote Imaging, Sensing and Processing (CRISP). 5-9 Nov. Vol 2: 813-818.

UNGANAI L.S. and KOGAN F.N., 1998, Drought Monitoring and Corn Yield estimation in Southern Africa from AVHRR Data. *Remote Sensing of Environment* **63**: 219-232.

WEISS J.L., GUTZLER D.S., COONROD J.E.A.and DAHM C.N., 2004, Long-term vegetation monitoring with NDVI in a diverse semiarid setting, central New Mexico, USA. *Journal of Arid Environments* **58.2** 249-272.